

Frequency synchronization of Fourier domain harmonically mode locked fiber laser by monitoring the supermode noise peaks

Feng Li,¹ Ai Qin Zhang,² Xinhuan Feng,^{2,*} and P. K. A. Wai¹

¹Photonics Research Centre, Department of Electronic and Information engineering, The Hong Kong Polytechnic University, Hong Kong

²Institute of Photonics Technology, Jinan University, Guangzhou, 510632, China
*eexhfeng@gmail.com

Abstract: In a harmonically mode locked laser, the supermode noise peaks in the RF spectrum can be observed directly because they are separated from the driving frequency and its harmonics of the active mode locker. Using a simple theoretical model, we showed that the intensities of the supermode noise peaks will decrease if the coherence of the laser output decreases. We harmonically mode locked a Fourier domain mode locked (FDML) fiber laser to the third order. We observed that the supermode noise peak intensities decrease significantly when the detune between the sweeping frequency of the tunable filter and the cavity resonant frequency increases. It is therefore possible to use the supermode noise peaks to monitor the frequency detune of the tunable filter for auto-calibration of FDML fiber lasers.

©2013 Optical Society of America

OCIS codes: (140.3600) Lasers, tunable; (140.4050) Mode-locked lasers.

References and links

1. R. Huber, M. Wojtkowski, and J. G. Fujimoto, "Fourier Domain Mode Locking (FDML): A new laser operating regime and applications for optical coherence tomography," *Opt. Express* **14**(8), 3225–3237 (2006).
2. S. W. Huang, A. D. Aguirre, R. A. Huber, D. C. Adler, and J. G. Fujimoto, "Swept source optical coherence microscopy using a Fourier domain mode-locked laser," *Opt. Express* **15**(10), 6210–6217 (2007).
3. R. Huber, D. C. Adler, V. J. Srinivasan, and J. G. Fujimoto, "Fourier domain mode locking at 1050 nm for ultra-high-speed optical coherence tomography of the human retina at 236,000 axial scans per second," *Opt. Lett.* **32**(14), 2049–2051 (2007).
4. L. Huo, J. Xi, K. Hsu, and X. Li, "OCT Imaging with discrete-frequency Fourier domain mode-locked laser," in *Biomedical Optics and 3-D Imaging* (2010), paper BSuC6.
5. K. Murari, J. Mavadia, J. Xi, and X. Li, "Self-starting, self-regulating Fourier domain mode locked fiber laser for OCT imaging," *Biomed. Opt. Express* **2**(7), 2005–2011 (2011).
6. D. Chen, C. Shu, and S. He, "Multiple fiber Bragg grating interrogation based on a spectrum-limited Fourier domain mode-locking fiber laser," *Opt. Lett.* **33**(13), 1395–1397 (2008).
7. H. D. Lee, E. J. Jung, M. Y. Jeong, and C. S. Kim, "Linearized interrogation of FDML FBG sensor system using PMF Sagnac interferometer," *Proc. SPIE* **7503**, 750355 (2009).
8. B. C. Lee and M. Y. Jeon, "Remote fiber sensor based on cascaded Fourier domain mode-locked laser," *Opt. Commun.* **284**(19), 4607–4610 (2011).
9. L. A. Kranendonk, X. An, A. W. Caswell, R. E. Herold, S. T. Sanders, R. Huber, J. G. Fujimoto, Y. Okura, and Y. Urata, "High speed engine gas thermometry by Fourier-domain mode-locked laser absorption spectroscopy," *Opt. Express* **15**(23), 15115–15128 (2007).
10. W. Wieser, B. R. Biedermann, T. Klein, C. M. Eigenwillig, and R. Huber, "Ultra-rapid dispersion measurement in optical fibers," *Opt. Express* **17**(25), 22871–22878 (2009).
11. W. Wieser, B. R. Biedermann, T. Klein, C. M. Eigenwillig, and R. Huber, "Multi-megahertz OCT: High quality 3D imaging at 20 million A-scans and 4.5 GVoxels per second," *Opt. Express* **18**(14), 14685–14704 (2010).
12. B. R. Biedermann, W. Wieser, C. M. Eigenwillig, T. Klein, and R. Huber, "Dispersion, coherence and noise of Fourier domain mode locked lasers," *Opt. Express* **17**(12), 9947–9961 (2009).
13. C. Jirauschek, B. Biedermann, and R. Huber, "A theoretical description of Fourier domain mode locked lasers," *Opt. Express* **17**(26), 24013–24019 (2009).
14. B. Howley, Z. Shi, Y. Jiang, and R. T. Chen, "Thermally tuned optical fiber for true time delay generation," *Opt. Laser Technol.* **37**, 29–32 (2005).
15. M. Becker, D. J. Kuizenga, and A. Siegman, "Harmonic mode locking of the Nd:YAG laser," *IEEE J. Quantum Electron.* **8**(8), 687–693 (1972).

16. N. Onodera, "Supermode beat suppression in harmonically mode-locked erbium-doped fibre ring lasers with composite cavity structure," *Electron. Lett.* **33**(11), 962–963 (1997).
17. F. Rana, H. L. T. Lee, R. J. Ram, M. E. Grein, L. A. Jiang, E. P. Ippen, and H. A. Haus, "Characterization of the noise and correlations in harmonically mode-locked lasers," *J. Opt. Soc. Am. B* **19**(11), 2609–2621 (2002).
18. O. Pottiez, O. Deparis, K. Roman, M. Haelterman, P. Emplit, P. Mégret, and M. Blondel, "Supermode noise of harmonically mode-locked erbium fiber lasers with composite cavity," *IEEE J. Quantum Electron.* **38**(3), 252–259 (2002).
19. K. Xu, R. Wang, Y. Dai, F. Yin, J. Li, Y. Ji, and J. Lin, "Supermode noise suppression in an actively mode-locked fiber laser with pulse intensity feed-forward and a dual-drive MZM," *Laser Phys. Lett.* **10**(5), 055108 (2013).
20. S. Slepneva, B. Kelleher, B. O'Shaughnessy, S. P. Hegarty, A. G. Vladimirov, and G. Huyet, "Dynamics of Fourier domain mode-locked lasers," *Opt. Express* **21**(16), 19240–19251 (2013).

1. Introduction

Recently Fourier domain mode locked (FDML) fiber lasers [1] have attracted much interest because of promising applications in optical coherence tomography (OCT) [2–5], optical fiber sensing [6–8], bio-chemical spectroscopy [9,10], and other optical systems requiring swept laser sources. Compared with conventional wavelength swept lasers with short cavities, FDML fiber lasers use a long cavity such that the repetition rate of the cavity equals to the sweeping rate of the tunable filter. With the synchronization, the sweeping rate of the frequency filter can be increased significantly from less than 100 kHz to several MHz because the sweeping rate is no longer limited by the laser build-up time [1,11].

The output quality of an FDML fiber laser, especially its coherence and linewidth, is limited by the fiber dispersion, modulation detune, and nonlinear effects [12]. The fiber dispersion in such broad spectral range will introduce significant time delay between the signals at different wavelengths after propagation in the kilometers long fiber of the cavity. Thus dispersion shifted fiber (DSF) or dispersion compensation fiber (DCF) is normally used in the cavity to minimize the total dispersion of the cavity.

FDML fiber lasers are very sensitive to the detune of the sweeping frequency of the tunable filter [13]. If the sweeping frequency is detuned from the resonant frequency of the cavity even by a few hundredth of a percentage of the cavity resonant frequency, the frequency mismatch will lower the coherence of the light in the cavity, and hence will decrease the FDML fiber laser output quality. In experiments, the synchronization between the sweeping frequency and the cavity resonant frequency is monitored typically through measuring the optical spectra and/or waveforms of the laser output. However, determining the frequency detune by using the optical spectra and/or waveforms of the laser output is not straightforward because they are not easy to be quantified.

Even after the sweeping frequency is perfectly tuned to the cavity resonant frequency, the synchronization can be easily broken by changes in fiber length such as those induced by the fluctuation in ambient temperature. For example, in a cavity with a resonant frequency of 200 kHz, a typical refractive index thermal coefficient of 10^{-5} K^{-1} , and an optical fiber thermal expansion coefficient of $5 \times 10^{-7} \text{ K}^{-1}$ [14], the cavity resonant frequency will vary with the temperature at the coefficient 1.46 HzK^{-1} . That means, a few degrees of variation in the temperature is sufficient to destroy the synchronization of the FDML fiber laser which will significantly decrease the signal quality. It is therefore important to develop a simple method to monitor the laser output quality and provide feedback for the synchronization of the sweeping frequency of the tunable filter in the instrumentation of FDML fiber lasers.

In a fundamentally mode locked FDML fiber laser, the beating signals in the radio frequency (RF) spectra induced by the correlation of the output from different round trips are superimposed with the modulation peaks of the swept filter [12]. In a harmonically mode locked FDML fiber laser, however, the modulation peaks appear only at the integral multiples of the sweeping frequency. Thus the beating signals, called supermode noise peaks, which appear at integral multiples of the cavity resonant frequency, can now be observed directly. We note that if the sweeping frequency of the tunable filter is detuned slightly from the laser cavity resonant frequency, the coherency of the cavity modes and that of the beating between the supermodes will decrease. Consequently, the supermode noise peaks will decrease. At

large frequency detune, the supermode noise peaks will disappear completely. In this paper, we show that monitoring the supermode noise peaks in the laser RF spectrum of a harmonically mode locked FDML fiber laser provides a straightforward method to monitor the laser output quality, hence the synchronization of the FDML fiber lasers. We demonstrated, to the best of our knowledge, for the first time an FDML fiber laser harmonically mode locked to the third order. We showed that even when the sweeping frequency of the tunable filter deviates from the cavity resonant frequency by less than 0.04%, the supermode noise peak is decreased by more than 18 dB.

2. Principle and theoretical model

Supermode noise in harmonically mode locked lasers has been discussed extensively [15–19]. In a laser harmonically mode locked to the N -th order, the lasing cavity supports N sets of phase locked cavity modes, called supermodes. If no special mechanism is used to suppress the unwanted supermodes, all of them will lase and the relative phases between the supermodes vary randomly. The beatings between these supermodes introduce intensity fluctuation between the consecutive pulses in the output of the harmonically mode locked laser. Different methods have been proposed to reduce the intensity fluctuation which include adopting a composite cavity to select only one set of the supermodes [16,18], using adaptive loss compensation [19], etc.

In a harmonically mode locked FDML fiber laser, if the sweeping frequency is detuned $\Delta\nu$ from the cavity resonant frequency f_{cav} , then at any wavelength λ within the sweeping range Θ of the tunable filter which is assumed to be driven by a symmetric triangular wave, the instantaneous central wavelength of the passband of the tunable filter will be shifted $\sim 2\Theta\Delta\nu/f_{\text{cav}}$ away from λ after every successive cavity round trip time. Thus even if the central frequency of the tunable filter is initially located at wavelength λ , the light at λ will experience increasing loss after every trip it travels around the cavity. The increase in the effective loss at λ means that the intensity of the laser light already built up at λ will decrease, and at the same time it will also be harder for new laser light to be built up from ASE noise. Since the transmission of the tunable filter remains the same, only its central wavelength location shifted, the relative portion of the ASE noise transmitted by the filter will increase. The coherence of the FDML fiber laser output will therefore decrease.

If an FDML fiber laser is harmonically mode locked at the N -th order, the laser output can be written as

$$E(t) = \sum_{k=1}^N A_k e^{i\psi_k} \left(\sum_{m=0}^{M-1} B_{Nm+k} e^{i\phi_{Nm+k}} e^{-i2\pi f_{Nm+k}t} \right), \quad (1)$$

where $k = 1, 2, \dots, N$ is the index of the supermodes and $m = 0, 1, \dots, M-1$ is the index of the $N \times M$ cavity modes in the N supermodes. The coefficient $A_k \exp(i\psi_k)$, where A_k is the amplitude and ψ_k is the phase, gives the mixing between the supermodes. Both A_k and ψ_k vary with time as the supermodes are not locked to each other. The expression in the parentheses on the right hand side of (1) represents the N supermodes where B_{Nm+k} , ϕ_{Nm+k} , and f_{Nm+k} are the mode amplitude, phase, and frequency respectively of the $(Nm+k)$ -th cavity mode which is part of the k -th supermode. Normally, B_{Nm+k} is defined by the passband profile of the tunable filter and ϕ_{Nm+k} are constant as the cavity modes of a supermode are phase-locked together.

The frequency detune will reduce the coherence of the cavity modes as well as the mixing between the supermodes. We assume that the decrease in coherence can be modeled by the random variations in the coefficients of the supermodes and cavity modes, i.e. the parameters A_k , ψ_k , B_{Nm+k} , and ϕ_{Nm+k} . To illustrate the effect of the decrease in coherence on the supermode noise peaks, we assume that both the phases ψ_k and ϕ_{Nm+k} are randomly varying, and for simplicity keep the amplitudes A_k and B_{Nm+k} constant in different round trips. For ψ_k , we assume

$$\psi_k^j = \psi_k^{j-1} + \text{rand}[-1,1]\Delta\psi_k, \quad \psi_k^0 = \text{rand}[-1,1]\pi, \quad (2)$$

where $j = 1, 2, \dots$ denotes the number of cavity round trips, $\Delta\psi_k$ is the strength of the phase variation of the k -th supermode, and the function $\text{rand}[-1,1]$ gives a random number between -1 and 1 with uniform distribution. Randomly chosen ψ_k^0 are used as the initial phases of the supermodes and the initial phases are kept the same in all samples while performing ensemble average. Equation (2) assumes that at every round trip the phases of the supermodes drift randomly from their values in the previous round trip.

The phase of the cavity modes is modeled simply as

$$\phi_{Nm+k}^j = \phi_{Nm+k}^0 + \text{rand}[-1,1]\Delta\phi_{Nm+k}, \quad (3)$$

where ϕ_{Nm+k}^0 and $\Delta\phi_{Nm+k}$ are the initial phase and the strength of the phase variation of the $(Nm + k)$ -th cavity mode. Thus the phases of the cavity modes are assumed to be perturbed from the initial phases (normally phase locked) in each round trip.

In the following discussion, we assume that the FDML fiber laser is harmonically mode locked to the third order, i.e. $N = 3$. For simplicity, we assume $\Delta\psi_k = \Delta\psi$, and $\Delta\phi_{3m+k} = \Delta\phi$ for $k = 1, 2$, and 3 , and $m = 0, 1, \dots, M-1$. In other words, we assume that all three supermodes have the same strength of phase variation $\Delta\psi$ and all $3M$ cavity modes have the same strength of the phase variation $\Delta\phi$. We further assume that all three supermodes have a Gaussian profile, $B_{3m+k} = \exp[-0.5(f_{3m+k}/\Lambda)^2]$, where $\Lambda = 20f_{\text{cav}}$. The amplitudes of the three supermodes are set to be identical, i.e. $A_k = 1$, $k = 1, 2, 3$. The supermodes are assumed to be initially unchirped, i.e. $\phi_{3m+k}^0 = 0$. The total number of cavity modes is chosen to be 1024. The numbers of cavity modes in the three supermodes therefore are not exactly the same. Since the frequency window is much larger than the bandwidth of the Gaussian profile, the intensities of the modes at the edge of the frequency window are negligible. The slight difference in mode number will not affect the results. The consecutive output from 256 cavity round trips is used to calculate the RF spectra.

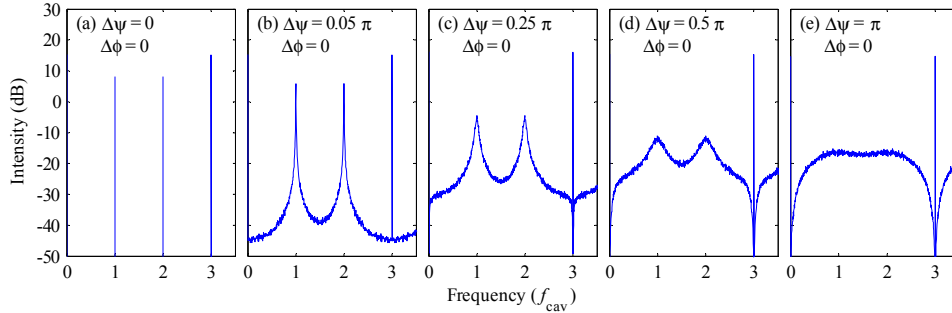


Fig. 1. The average RF spectra of signals defined in (1) with cavity mode phase variation $\Delta\phi = 0$ and supermode phase variation $\Delta\psi = 0, 0.05\pi, 0.25\pi, 0.5\pi$ and π . The RF spectra shown are the average of 100 random samples.

First we consider the effect of increase in random mixing of the supermodes. Thus we set $\Delta\phi = 0$. Figure 1 shows the RF spectra obtained with the signals in (1) for frequencies up to $3f_{\text{cav}}$. The RF spectra are obtained after ensemble average with 100 samples. Figures 1(a)–1(e) show the RF spectra for the strength of random phase $\Delta\psi = 0, 0.05\pi, 0.25\pi, 0.5\pi$ and π respectively. Figure 1(a) shows that without random phase mixing, i.e. $\Delta\psi = 0$, the beating of the supermodes give high supermode noise peaks at f_{cav} and $2f_{\text{cav}}$ and the harmonic resonant peak at $3f_{\text{cav}}$. Higher order supermode noise peaks can be observed at $(3p + 1)f_{\text{cav}}$ and $(3p + 2)f_{\text{cav}}$ and higher order harmonic resonant peaks can be observed at $3(p + 1)f_{\text{cav}}$ where $p = 1, 2, \dots, M-1$. When $\Delta\psi$ is increased from 0 to π , Figs. 1(a)–1(e) show that the supermode noise

peaks decrease from 8 dB to the noise floor at -16 dB. The noise floor increases from -45 dB at $\Delta\psi = 0.05\pi$ to -16 dB at $\Delta\psi = \pi$. The linewidth of the supermode noise peaks also increases. When $\Delta\psi = \pi$, which means the relative phases of the supermodes are completely randomized between successive roundtrips, there are no longer any supermode noise peaks in the RF spectrum. The intensity of the harmonic resonant peak at $3f_{\text{cav}}$, on the other hand, remains unchanged when $\Delta\psi$ varies from 0 to π . Thus the contrast between the harmonic resonant peak at $3f_{\text{cav}}$ and the supermode noise peaks at f_{cav} and $2f_{\text{cav}}$ increases when the mixing between supermodes is randomized.

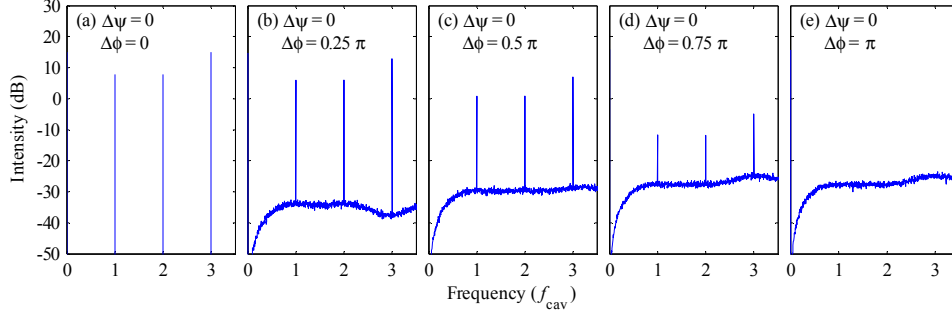


Fig. 2. The average RF spectra of signals defined in (1) with supermode phase variation $\Delta\psi = 0$ and cavity mode phase variation $\Delta\phi = 0, 0.25\pi, 0.5\pi, 0.75\pi$ and π . The RF spectra shown are the average of 100 random samples.

Next we study the effect of decrease in the coherence of cavity modes. We therefore set $\Delta\psi = 0$. Figures 2(a)–2(e) show the RF spectra for $\Delta\phi = 0, 0.25\pi, 0.5\pi, 0.75\pi$ and π , respectively. We observed that when $\Delta\phi$ increases from 0 to π , the intensities of the supermode noise peaks at f_{cav} and $2f_{\text{cav}}$ and the harmonic resonant peak at $3f_{\text{cav}}$ drop simultaneously. The difference between the supermode noise peaks and the harmonic resonant peak remain roughly the same. Unlike the increase of $\Delta\psi$ studied in Fig. 1, the linewidths of the supermode noise peaks do not increase when $\Delta\phi$ increases from 0 to π . While the noise floor increases significantly when $\Delta\phi$ changes from 0 (noiseless case) to 0.25π , it does not vary much when $\Delta\phi$ changes from 0.25π to π . When $\Delta\phi = \pi$, the supermode noise peaks and the harmonic resonant peak disappear as the cavity modes are completely randomized.

It is important to emphasize that the conditions $\Delta\psi = 0$ and $\Delta\phi = 0$ do not correspond to the optimal operation point of the laser. It only gives the condition that the sweeping frequency is synchronized with the cavity resonant frequency such that the cavity modes and the mixing of the supermodes are coherent and stable. The supermode noises remain, as shown in Figs. 1(a) and 2(a). The extent of the beating between the supermodes, hence the amplitude jitters, depend on their initial phase ψ_k^0 . Different choices of ψ_k^0 will lead to different correlation of the pulses in the laser cavity. For some special sets of ψ_k^0 the supermode noise peaks will disappear completely because of the destructive interference among the supermodes. The laser output is optimal because it is without phase noise and supermode noise. In general, when both the amplitude noise and phase noise of the supermodes and cavity modes are zero, there are more than one choices of $A_k^0, \psi_k^0, B_{Nm+k}^0$, and ϕ_{Nm+k}^0 such that the supermode noise are also zero, i.e. the optimal operation point of the laser is not unique. The function of supermode noise suppression schemes [16,18,19] is to render the laser to operate near one of these optimal points.

For the example of the third order harmonically mode locked laser considered above, the specific initial phase values of ψ_k^0 for minimum supermode noise peaks are

$(\psi_1^0, \psi_2^0, \psi_3^0) = (0, 0, \pm 2\pi/3)$ or its permutations. The three pulses in the cavity have identical intensity and the supermode noise peaks on the RF spectrum are suppressed completely. When $(\psi_1^0, \psi_2^0, \psi_3^0)$ deviates from $(0, 0, \pm 2\pi/3)$, e.g.

$$\psi_k^0 = \bar{\psi}_k^0 + \text{rand}[-1, 1]\delta\psi_k \quad (4)$$

where $\delta\psi_k$, $k = 1, 2, 3$ is the amplitude of the random variation of the initial phase, and $(\bar{\psi}_1^0, \bar{\psi}_2^0, \bar{\psi}_3^0) = (0, 0, \pm 2\pi/3)$, the supermode noise peaks reappear in the RF spectra. Figure 3 shows the average RF spectra at different $\delta\psi_k$, where for simplicity we have assumed $\delta\psi_k = \delta\psi$ for $k = 1, 2, 3$, $\Delta\psi = 0$, and $\Delta\phi = 0$. The RF spectra shown are the average of 100 random samples. The supermode noise peaks increase rapidly with $\delta\psi$. We note the absence of noise floor in Fig. 3. The phase deviation $\delta\psi_k$ from $\bar{\psi}_k^0$ leads to variation in the amplitude of the supermode noise peaks but do not create any new frequency component as ψ_k does not change from round trip to round trip.

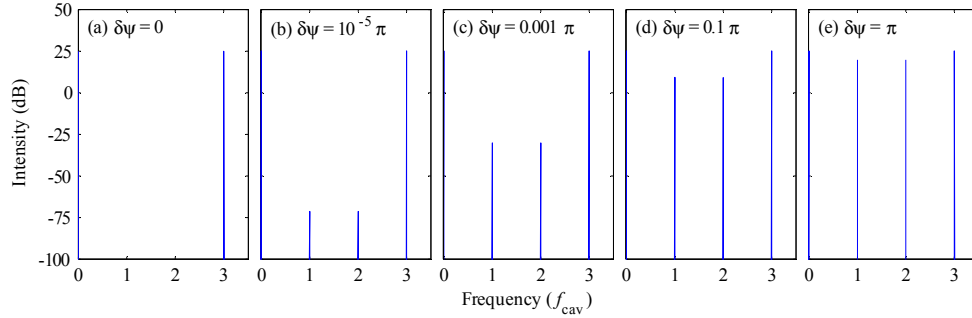


Fig. 3. The average RF spectra of signals defined in (1) with $\Delta\psi = 0$, $\Delta\phi = 0$ and $\delta\psi = 0, 10^{-5}\pi, 0.001\pi, 0.1\pi$, and π . Each of the RF spectra shown is the average of 100 random samples.

In [17], Rana et al. related the supermode noise peaks of the RF spectrum with the decorrelation of noise among the pulses inside the laser cavity. They observed that if the noise in all the pulses in the laser cavity is completely positively correlated, then the supermode noise peaks will disappear. If the uncorrelated noise like ASE increases, the supermode noise peaks will re-appear and then increase. Since Rana et al. studied the effect of noise on an identical pulse train spaced regularly apart, they studied the effect of pulse noise when the laser operates at one of the optimal points at which the amplitude noise and phase noise of the supermode and cavity modes, and the supermode noise peaks are zero. Thus when uncorrelated noise like ASE increases, the supermode noise peak will increase in analogous to Fig. 3. We studied the effect of the change in ASE noise when the laser is assumed to be near but not at these optimal operation points. Thus when the ASE noise is increased, the supermode noise peaks are reduced and eventually disappear as shown in Figs. 1 and 2.

To summarize, in order to achieve optimal operation of a harmonically mode locked FDML fiber laser, the sweeping frequency should first be tuned to synchronize with the cavity resonant frequency. When the frequencies are far away from synchronization, there is no supermode noise peak and the noise floor in the RF spectrum is high, similar to that shown Figs. 1(e) or 2(e). When the frequencies are near synchronization, without any supermode noise suppression mechanism in the cavity, the supermode noise peak will begin to grow as shown in Figs. 1(d)–1(b) or 2(d)–2(b). The supermode noise peaks can now serve as a useful indicator to synchronize the frequencies. The laser is considered synchronized when the supermode noise peaks are maximized as shown in Figs. 1(a) or 2(a). At this point, mechanisms to suppress the supermode noises should be turned on to render the laser to operate at one of the optimal points, Figs. 3(a)–3(e).

We note that the above analysis is not confined to FDML fiber lasers. It can be applied to any harmonically mode locked lasers in which the signal quality, especially coherence, is reduced by the mismatch or misalignment of some cavity parameters, such as the case of frequency detuning in FDML fiber lasers.

3. Experimental setup

We then carried out an experiment on harmonically mode locked FDML fiber laser to study the effect of frequency detuning on the supermode noise peaks. Figure 4 shows the schematic of an FDML fiber laser. The ring cavity consists of a semiconductor optical amplifier (SOA, manufactured by CIP) as the gain medium, an isolator (ISO) to ensure unidirectional operation, a fiber Fabry-Pérot tunable filter (FFP-TF, manufactured by Micron Optics) driven by a swept driver for wavelength selection, a 90/10 coupler to output 10% of the power from the laser cavity and feedback the remaining light into the SOA, and a delay line of ~4.7 kilometers long dispersion shifted fiber (DSF) which sets the cavity resonant frequency to about 43 kHz.

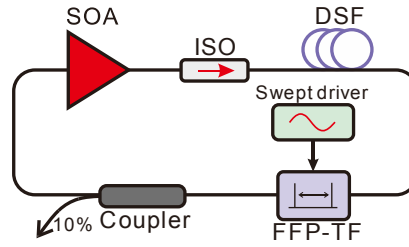


Fig. 4. Schematic of an FDML fiber laser. The cavity is comprised of a semiconductor optical amplifier (SOA), an isolator (ISO), a section of dispersion shifted fiber (DSF), a fiber Fabry-Pérot tunable filter (FFP-TF) driven by a swept driver, and a coupler to output the signal.

The SOA has a small signal gain of 20 dB at a central wavelength of 1550 nm and 3 dB bandwidth of 60 nm with a bias current of 70 mA. The FFP-TF is driven by a continuous sinusoidal signal generated by the swept driver. The amplitude of the sinusoidal signal is

$$V(t) = V_{\text{amp}} \times \sin(2\pi f_{\text{drive}} t) + V_{\text{bias}}, \quad (5)$$

where V_{amp} is the driving amplitude which determines the swept range of the spectrum, V_{bias} is the bias voltage used to set the central wavelength of the swept range, and f_{drive} is the driving frequency of the tunable filter, also called sweeping frequency. In the experiment, f_{drive} is carefully tuned to be integral multiples of the cavity resonant frequency f_{cav} to achieve Fourier domain mode locking.

The integrated spectra of the output signal are measured by an optical spectrum analyzer. The signal is also converted to electrical signal by a photo-detector and then the waveforms and RF spectra are measured by an oscilloscope and an electrical spectrum analyzer respectively with the electrical signal.

4. Results and discussion

In the experiment, the resonant frequency of the cavity f_{cav} is estimated by the cavity length as

$$f_{\text{cav}} = \frac{c}{n \times l_{\text{cav}}}, \quad (6)$$

where n is the effective refractive index of the fiber, l_{cav} is the total cavity length, and c is the speed of light in vacuum. The length of the fiber pigtailed of the optical components in the cavity cannot be measured precisely and the total length is estimated to ~20 m. We use the total cavity length ~4.72 km and the effective refractive index of the DSF $n = 1.473$ to estimate f_{cav} as ~43.1 kHz. So the corresponding harmonic mode locking frequencies will be

$N \times 43.1$ kHz, where $N > 1$ is an integer. The sweeping frequency of the FFP-TF is limited by the response spectrum of the FFP-TF. Owing to the intrinsic response of the piezoelectric material used in the FFP-TF, an FFP-TF typically can only work well near several frequency peaks. For the FFP-TF used in this experiment, the response peaks are near 43 kHz and 129 kHz which can be used to drive the fundamental and third harmonic mode locking in the same FDML fiber laser cavity.

4.1 Fundamental mode locking

The repetition rate of the swept driver is initially set to the estimated resonant frequency 43.1 kHz. The driving amplitude V_{amp} is set to 100 mV which will generate about 42 nm swept range. The swept range is not optimized. A typical value is chosen merely to illustrate that the sweeping frequency overlaps with the cavity resonant frequency on the RF spectrum for a fundamentally mode locked laser. The swept range can be easily extended by increasing the driving amplitude without affecting the RF spectrum significantly. The sweeping frequency is adjusted to synchronize with the cavity resonant frequency by optimizing the integrated output spectrum as shown in Fig. 5(a). The signal-to-noise ratio (SNR), which is defined as the difference in logarithmic scale of the minimum intensity inside the swept range and the maximum intensity outside the swept range, will be measured from the integrated spectrum. The integrated output spectra have peaks at the borders of the spectrum because the sweeping speed has the minimum at the spectrum borders while the filter is driven by a sinusoidal signal. The detune of the sweeping frequency will introduce higher loss on the resonant signals which satisfy the cavity resonant condition. The extra loss will suppress the coherent part of the resonant signal and replenish the signal by amplifying the residual signals which are dominant by spontaneous emissions. The maximum SNR of 16.6 dB is observed at the sweeping frequency of 43.041 kHz. The SNR decreases when the sweeping frequency is detuned from 43.041 kHz. The SNR decreases to 9.1 dB at detune of ± 20 Hz, which is a drop of 7.5 dB from the maximum SNR value for detune of only 0.046% from the optimal value. Figure 5(b) shows the output waveforms of the synchronized and slightly detuned sweeping frequencies. We observed that the output waveforms are sensitive to the detune of sweeping frequency. Thus synchronization between the sweeping frequency and the cavity resonant frequency is crucial to the output signal quality.

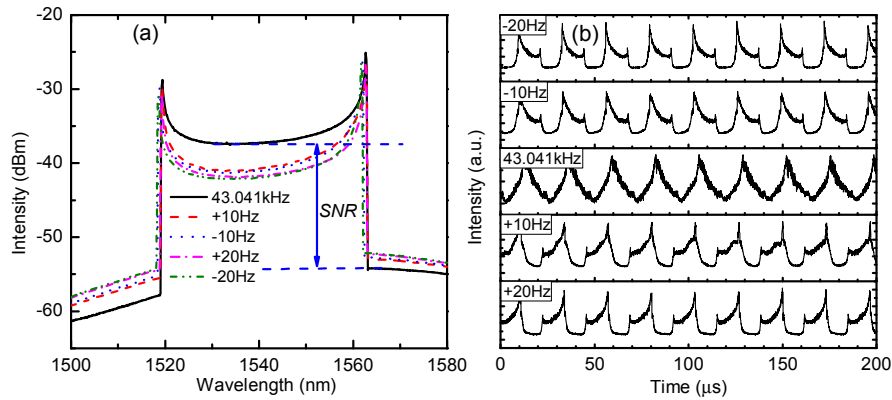


Fig. 5. (a) Integrated spectra and (b) waveforms from the fundamentally mode locked FDML fiber laser with different detunes for $V_{\text{amp}} = 100$ mV. The sweeping frequency of the FFP-TF is 43.041 kHz and relative detunes are ± 10 Hz, and ± 20 Hz.

In an FDML fiber laser mode locked at the fundamental mode, the cavity resonant frequency in the RF spectrum is superimposed on the driver frequency [12]. Figure 6 shows the RF spectra of the output signals while the sweeping frequency is detuned from 0 to 40 Hz. Figure 6(a) shows the RF spectra from 0 to 300 kHz and Fig. 6(b) shows the zoom-in detail in the range 30 to 60 kHz. From Fig. 6(b), the intensity of the RF spectral peaks near the

resonant frequency 43.041 kHz varies about only 1.6 dB when the frequency is detuned by 40 Hz.

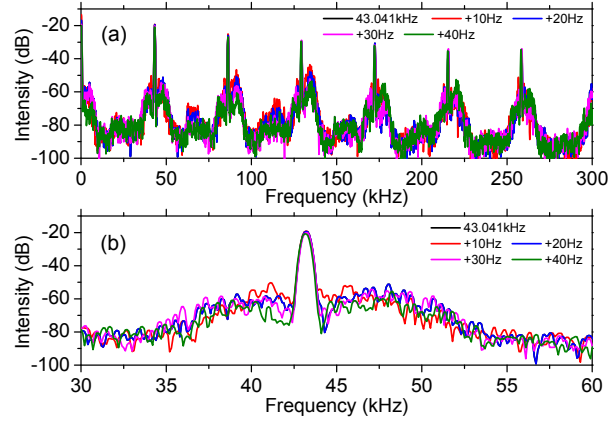


Fig. 6. The RF spectra of the fundamentally mode locked FDML fiber laser output signals with sweeping frequency detunes of 0 (black), 10 (red), 20 (blue), 30 (magenta), and 40 Hz (green).

4.2 Third harmonic mode locking

To separate the superimposed cavity resonant frequency and sweeping frequency, we drive the tunable filter at the third harmonic frequency to mode lock the FDML fiber laser at the third harmonic. As the cavity resonant frequency is 43.041 kHz, the sweeping frequency to realize the third harmonic mode locking in the same cavity should be close to 129.123 kHz. By optimizing the *SNR* in the integrated output spectrum, stable harmonic mode locking in the FDML fiber laser is obtained at the driver frequency of 129.125 kHz. The driving amplitude V_{amp} is 500 mV which generates more than 80 nm swept range.

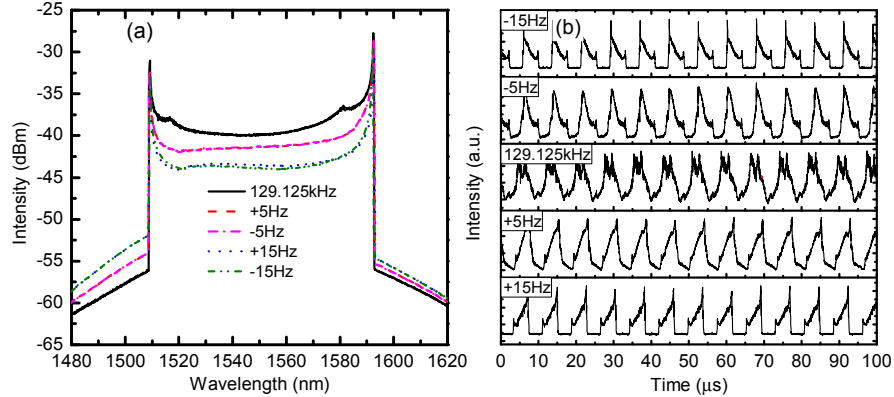


Fig. 7. (a) The integrated spectra and (b) waveforms of the FDML fiber laser harmonically mode locked at the third order for $V_{amp} = 500$ mV. The scan frequency of the FFP-TF is 129.125 kHz and relative detunes are ± 5 Hz, and ± 15 Hz.

Figure 7(a) shows the integrated output spectra at 129.125 kHz and relative detunes of ± 5 Hz and ± 15 Hz. The *SNR* drops from 15.7 dB at 129.125 kHz to 7.6 dB when the detune is increased to 15 Hz. Figure 7(b) shows the corresponding output waveforms. Similar to the results shown in Fig. 5(b), detune in the sweeping frequency will induce strong asymmetry on the waveforms caused by the detuning and the linewidth enhancement factor of the SOA [13, 20]. The output waveforms of the third order harmonically mode locked fiber laser at the synchronized sweeping frequency are somewhat different to that of the fundamental mode

locking. There are two peaks in a single swept round trip due to the broader swept range in spectrum.

Figure 8 shows the RF spectra of the third harmonically mode locked FDML fiber laser. Figures 8(a)–8(c) show the RF spectra at different scales. Figures 8(b) and 8(c) show the RF spectra in small regions around the sweeping frequency and the cavity resonant frequency. From Fig. 8(a), the noise floor in the low frequency region is about -90 dB for all the data shown. Small peaks, at intensities less than -15 dB below the supermode noise peak, are observed roughly between the harmonics of the cavity resonant frequency. These small peaks are likely caused by the imperfection of the driving signal, the response curve of the piezoelectric transducer based tunable filter, the gain dynamics of the SOA, and/or the nonlinearity of the elements in the long cavity. The intensities of the dominant mode at the sweeping frequency and the first supermode noise peak reach the maximum values at -27.3 and -57 dB, respectively at the sweeping frequency of 129.125 kHz. But their values drop to -31.1 and -75 dB respectively when the sweeping frequency is detuned by -15 Hz. In other words, the mode peak at the sweeping frequency is decreased by only 3.8 dB, but the first supermode noise peak is decreased by 18 dB for a detune of only 0.012% of the optimal sweeping frequency.

Figure 9 shows the peak intensities of the RF spectra in Figs. 8(b) and 8(c) versus the detune of sweeping frequency. Thus the intensity of the supermode noise peak is much more sensitive to the frequency detune than that at the sweeping frequency.

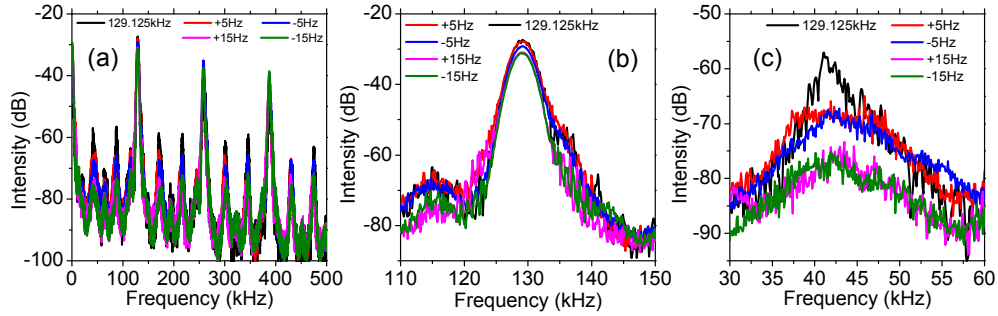


Fig. 8. The RF spectra of the FDML fiber laser with sweeping frequency at 129.125 kHz and relative detunes of ± 5 Hz and ± 15 Hz.

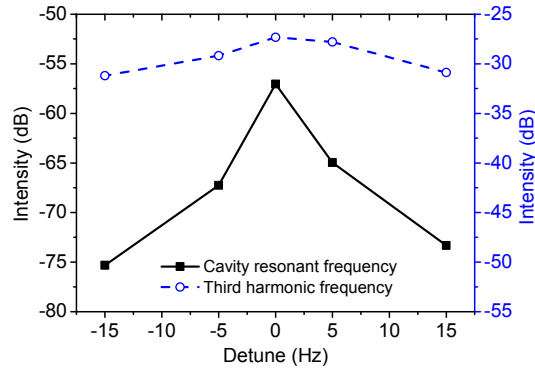


Fig. 9. The peak intensities of the RF spectra at the third harmonic frequency (solid squares) and the cavity resonant frequency (open circles) versus frequency detune.

5. Conclusion

In this paper, we studied the effect of frequency detune on the supermode noise peaks of a harmonically mode locked fiber laser. We observed that detune between the sweeping frequency of the tunable filter and the cavity resonant frequency will lower the coherency of the FDML fiber laser output. We assume that such decrease in coherence of the laser output can be modeled by the increase in randomization of the mixing between the supermodes and/or the randomization of the cavity modes inside the supermodes. Using a simple theoretical model, we showed that the intensity of supermode noise peaks will decrease if the random mixing of the supermodes or the cavity modes increase. Thus the supermode noise peaks, which can be measured directly from the RF spectrum, can be used as a measure of the coherency of FDML fiber laser output. The FDML fiber laser can be assumed to be synchronized when the supermode noise peaks are at the maximum.

We demonstrated for the first time an FDML fiber laser harmonically mode locked to the third order at a repetition rate of 129 kHz. The cavity resonant frequency is 43 kHz. By adopting harmonic mode locking, the frequency components corresponding to the sweeping frequency of the tunable filter were shifted away from supermode noise peaks, which are at integral multiples of the cavity resonant frequency. In the experiments, when the sweeping frequency is detuned by 15 Hz from the optimum value, the supermode noise peak drops by 18 dB from -57 to -75 dB. The change in the supermode noise peaks can therefore be used as feedback to synchronize the tunable filter by dynamically adjusting the sweeping frequency, which will enable auto-calibration of FDML fiber lasers.

It is important to point out that when the FDML fiber laser is synchronized by the proposed scheme, the laser is not operating optimally because the supermode noises are at the maximum. For optimal operation of the FDML fiber lasers, the supermode noise should also be suppressed. One way to suppress the supermode noise peaks in conventional harmonic mode locked lasers is to use specially designed cavities such that only one set of supermode survives [16, 18]. This approach, however, is not suitable for the proposed scheme as there will not be any supermode noise peaks to be utilized for the synchronization of the FDML fiber lasers. Active approach to reduce the amplitude noise which can be turned on after the FDML fiber laser is synchronized such as that proposed in [19] should be adopted.

Acknowledgments

This project was supported by the Hong Kong Research Grants Council General Research Fund (Grant No. PolyU 5263/13E). Xinhuan Feng acknowledges support by the NSFC (No. 61077030) and the Research Fund for the Doctoral Program of Higher Education of China (No. 20104401120009).